3D-Printed Ready-To-Use Variable-Stiffness Structures

Majid Taghavi, Tim Helps, Boxiong Huang, and Jonathan Rossiter

***Abstract*—Various physical phenomena have been used to develop variable-stiffness (VS) materials and structures, but all have involved some elements of manual fabrication, which limits their applications. In contrast, here we show fully three-dimensional (3D) printed monolithic VS structures that can be used directly from the printer. Thermally responsive polylactic acid (PLA) and conductive graphene PLA (GPLA) are combined in-printer to deliver a new framework for the temperature-controlled 3D VS structures. The embedded GPLA acts as a heating element, and both it and the surrounding PLA can be transitioned from rigid to soft using simple Joule heating because of the glass transition behavior of PLA. The mechanical and electrical properties of printed composite VS structures are studied. The great potential of this technology is demonstrated in a prototype variable-stiffness orthotic for foot drop.**

***Index Terms*—Compliance and impedance control, flexible robots, wearable robots, prosthetics and exoskeletons, rehabilitation robotics.**

I. Introduction

RECENTLY, variable-stiffness (VS) materials and structures have been demonstrated as a means of shape adaption [1] and transitioning between soft and rigid states [2]. They have a broad range of applications in robotics, particularly where compliant and safe motion are needed, ranging from robotic manipulation [3] to human-robot interactions [4], prosthetics [5] orthotics [6], and wearable [7] robots. They have great potential to be used in aircraft that undergo certain geometrical changes to enhance or adapt to their mission profiles [8],and they can be used in medicine (such as in endoscopes and colonoscopes to decrease the patient discomfort) [9]. Variable stiffness structures are often required for walking, hopping and running robots [10]–[12].

Different physical phenomena and engineering solutions have been applied to control material stiffness. In magnetorheological or electrorheological fluids, viscosity may be adapted by changing the orientation of nano/micro sized particles by subjecting them to magnetic and electric fields, respectively [13]. These smart materials are appropriate for fast switching requirements. However, they require sophisticated structures for fluid encapsulation and field generation. Phase changing materials, usually made of low melting point substances, serve as another category of VS materials. The stiffness is changed by environmental or direct Joule heating, and results in transition between solid and liquid phases, thus encapsulation is required [14]. These thermoactivated VS materials have low bandwidth and need sufficient time to transfer thermal energy into, and out of, the structure. Shape-memory alloys and shape-memory polymers (SMP) are a class of stimulus-responsive materials with the ability to undergo a large recoverable deformation upon external stimulus, such as heat, electricity, magnetism and application of solvent [15]. SMPs experience softening when they are heated above a glass transition temperature, T_g. They can be reshaped and will keep their new shape through a simple thermo-mechanical cycle. They automatically recover their original shape by reheating. However, most thermoplastic materials can be used as VS materials, changing the stiffness between a rigid and a soft, rubbery state when heated over their respective T_g. In this regard, PLA and ABS filaments have been used as VS elements where heating is achieved by external or embedded NiTi or NiCr wires [16], [17]. These VS fibers can be sewn into fabric, allowing a change in rigidly of entire wearable structures.

In this paper, we present a totally 3D-printable VS structure based on thermally responsive graphene PLA (GPLA) which acts as the heating element and is printed at the same time as, and in composition with, non-conductive PLA by means of multi-material 3D printer. This method employs a single-step fabrication process, where any desired 3D shape and configuration is achievable. The mechanical and electrical properties of the basic printed structures are studied, and we demonstrate that these 3D-printed VS elements have a great potential to be used in orthotics by demonstrating a foot drop splint.

II. Material and Methods

A. Design

Fig. 1 shows the main concept of the printed VS structure. A two-material 3D part is first designed where the GPLA material (which forms the heating elements) is encapsulated in the centre of larger PLA rods. In this way the central heater element is in direct contact with the structural PLA and ensures high efficiency in convective heat transfer. When current flows through the GPLA element, Joule heating occurs. Variation in stiffness

Manuscript received September 10, 2017; accepted February 7, 2018. Date of publication March 7, 2018; date of current version March 28, 2018. This letter was recommended for publication by Associate Editor A. Frisoli and Editor Y. Yokokohji upon evaluation of the reviewers' comments. This work was supported by the U.K. Engineering and Physical Sciences Research Council under Grants EP/M020460/1 and EP/M026388/1. *(Corresponding author: Jonathan Rossiter.)*

M. Taghavi, T. Helps, and J. Rossiter are with the Department of Engineering Mathematics and the Bristol Robotics Laboratory , University of Bristol, Bristol BS8 1UB, U.K. (e-mail: majid.taghavi@bristol.ac.uk; tim.helps@bristol.ac.uk; jonathan.rossiter@bris.ac.uk).

B. Huang is with the Department of Mechanical Engineering, University of Bristol, Bristol BS8 1UB, U.K. (e-mail: bh15077@bristol.ac.uk).

Digital Object Identifier 10.1109/LRA.2018.2812917

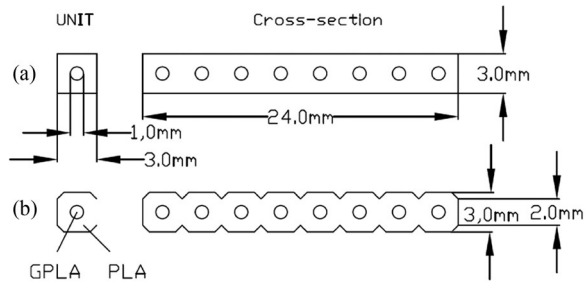

Fig. 1. Cross-section schematic showing encapsulated GPLA in PLA elements (left) and multi-element structures (right) for each of two VS structure types: (a) Type A and (b) Type B. Each fabricated sample was 100 mm in length.

results from heating because PLA exhibits glass transition behaviour, whereby above a certain temperature (59.2±1 °C for pure PLA [18]), it transitions from a hard to a soft state.

Graphene conductive PLA was selected as the heating element because it meets electrical, mechanical, and fabrication requirements. The comparatively low resistivity of GPLA ensures a large amount of heating can be achieved at a low voltage. In addition, GPLA has similar mechanical properties to the non-conducting PLA and the mechanical properties of the whole structure (at any given temperature) are therefore not significantly affected by the use of GPLA in place of PLA. Furthermore, the ability to simultaneously print both GPLA and PLA results in a fabrication process that is fast, simple and cost effective. A series of conductive parallel lines, which are electrically connected at each, are embedded in the structure for heating purposes.

As shown in Fig. 1, two different cross-sectional patterns were considered while the shape and size of the conductive lines were kept constant, i.e., circular cross section with 1 mm diameter. The first type is formed from a square cross section (Type A), whereby the GPLA core runs through a square section. Eight such squares are combined to yield a complete 24 by 3 mm structure. The second type features chamfered square cross sections around the heating element, which resemble a series of parallel cylinders connected laterally (Type B).

B. Fabrication

All characterized components were printed by means of multi-material 3D printer (Duplicator 4S, Wanhao, China). We used off-the-shelf PLA filament (832-0223, RS Components Ltd, UK) and conductive graphene PLA filament (GRPHN-PLA, Black Magic 3D, US), which had a volume resistivity of 0.6 ohm.cm. The GPLA begins to soften at a temperature of around 50 °C and the recommended extrusion temperature is 220 °C. Five test pieces of each of the VS structures (Type A and Type B) were fabricated and tested.

C. Experiments

The beam-shaped 3D-printed VS structures (dimensions 3 mm × 24 mm × 100 mm) were attached to a linear actuator (X-LSQ150B-E01, Zaber Technologies Inc., Canada) and a load cell (DBCR-10N-002-000, Applied Measurements, UK)

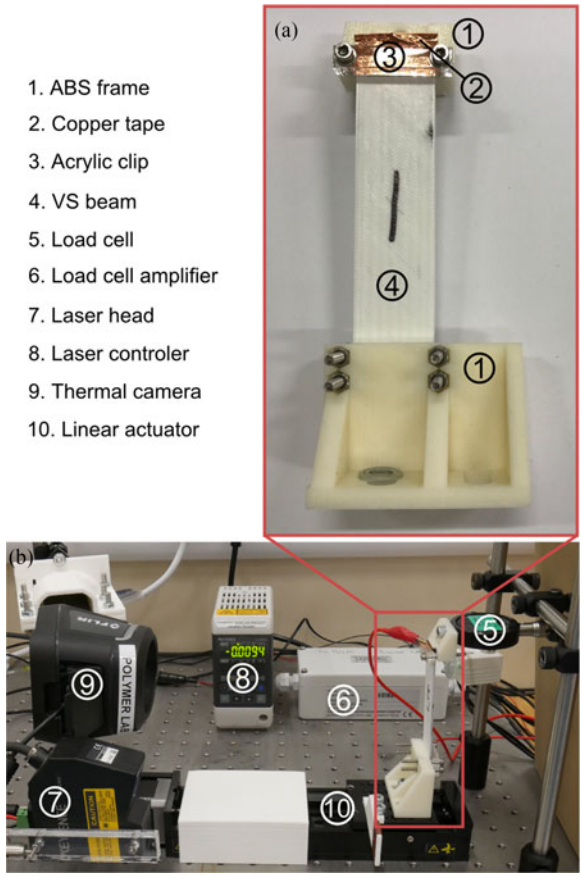

Fig. 2. (a) 3D-printed variable stiffness beam (Type A) attached to ABS test mounts. The conductive ends are connected to copper tape to ensure a good electrical connection. (b) VS beam connected to the actuator and load cell (right). A thermal camera captures the tempreture of the beam (top left). A laser dispalcement meter measures its displacement (bottom left).

at each end using 3D-printed ABS frames (Fig. 2(a)). The linear actuator (which was fixed on the steel breadboard) enforced cyclic, forward-backward movement while the force exerted by the other end of the VS component was measured by the load cell, as shown on Fig. 2(b). The amplitude of the linear driver movement was 4 mm and the period 4.2 s. A precision laser measurement system (LK-G152, Keyence, Japan) measured the real-time displacement of the sample. The output data from the load cell and laser measurement was collected by a data acquisition device (USB-6001, National Instruments, US).

The VS parts were heated by a current controlled DC power supply and the delivered current was set to 0.2 A. To obtain a reliable connection between wires and conductive PLA, the connections were made to copper tape, which was clamped against the ends of the VS structure by acrylic clips. A thermal camera (FLIR E4, FLIR, US) was used to measure the temperature of the sample.

III. Results and Discussion

Fig. 3 illustrates the typically recorded displacement, force and temperature as a function of time. As the deflection is enforced by the actuator to one end of the VS beam, the reaction force exerted is measured by the load cell at the other end. When

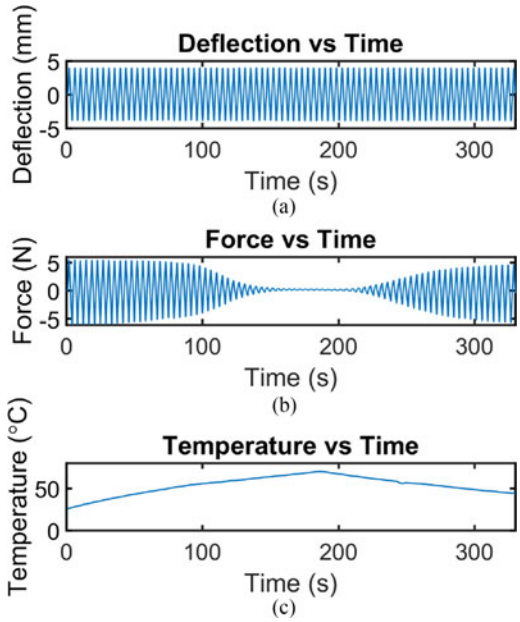

Fig. 3. (a) Actuator displacement measured by the laser displacement meter; (b) force exerted at the top of the VS structure measured by load cell; (c) temperature of the center of the beam measured by thermal camera.

the VS beam is rigid, it deforms elastically at a high stiffness and returns to its original shape (shown as high cyclic forcing in at the left and right of Fig. 3(b)). The material's response to the displacement is changed as it is heated. The beam becomes softer and consequently, stiffness reduces, and the reaction force is reduced. At a temperature that corresponds to glass transition temperature T_g of PLA (around 60 °C), the reaction force becomes close to zero, which means that the polymer is so soft that it is reshaped under external force (shown in the middle region of Fig. 3(b)).

In fact, beyond the glass transition temperature, deformation is plastic rather than elastic. The heating speed depends on several parameters such as applied current, total resistance of conductive GPLA elements, the shape and size of both conductive and nonconductive elements, and convective heat transfer around the structure. In the experiments described here, we heated the element over a cycle of roughly 300 seconds (around 150 s heating, 150 s cooling) and measured the mechanical properties of each test sample. Fig. 4 shows the snapshots of the video captured by the thermal camera. The number in the top left corner shows the temperature at the centre of the VS beam. The sensitivity to emission of the thermal camera was calibrated by heating the VS beam to known temperatures, in stages up to 65 C, thereby ensuring temperature measurement accuracy. MATLAB Optical Character Recognition was used to extract the corresponding temperature from each frame for use in analysis.

Synchronisation of the data acquisition device with the thermal camera was achieved using an LED, which was turned on (Fig. 4(a)) at the start of data capture. In this way, displacement, force and temperature were simultaneously measured with respect to time during experiments. The stiffness of the beam was calculated by dividing the maximum measured force by the peak

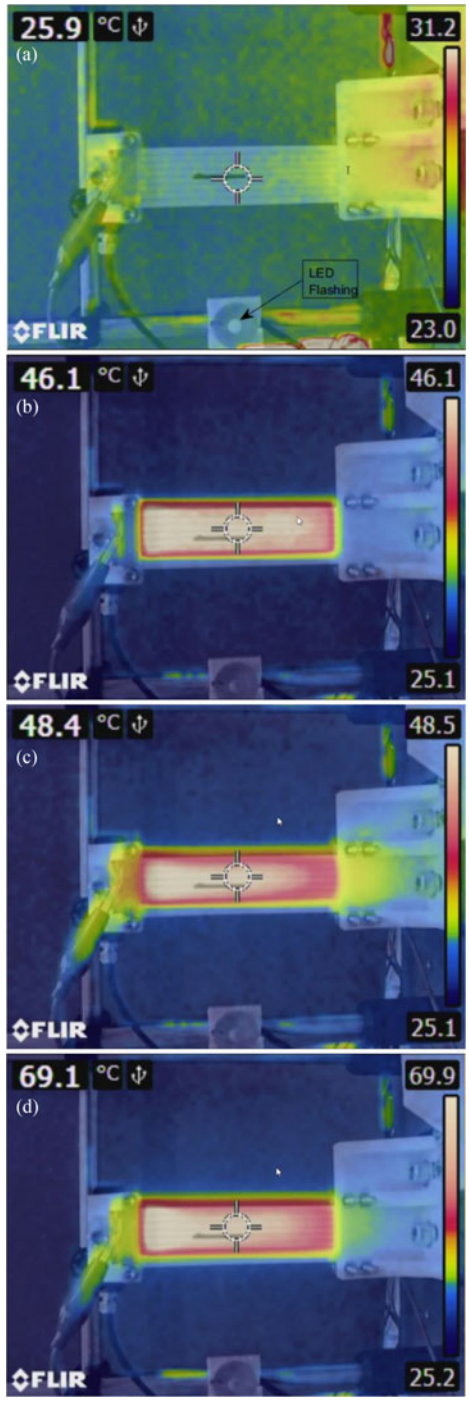

Fig. 4. Snapshots from the video taken by the thermal camera, The number at the top left shows the temperature of the centre point.

displacement for each cycle. The scatter plot in Fig. 5(a) shows stiffness variation with temperature for a test of a typical sample of a Type A structure. A 7th order polynomial best-fit (least squares) is shown on the graph as a smooth curve, which allows for simpler comparison of stiffness variation with other tests and samples. To reduce testing errors and determine if heating and reshaping influence the measured parameters, all 10 samples (5 of each type) were tested five times and no noticeable variation was observed.

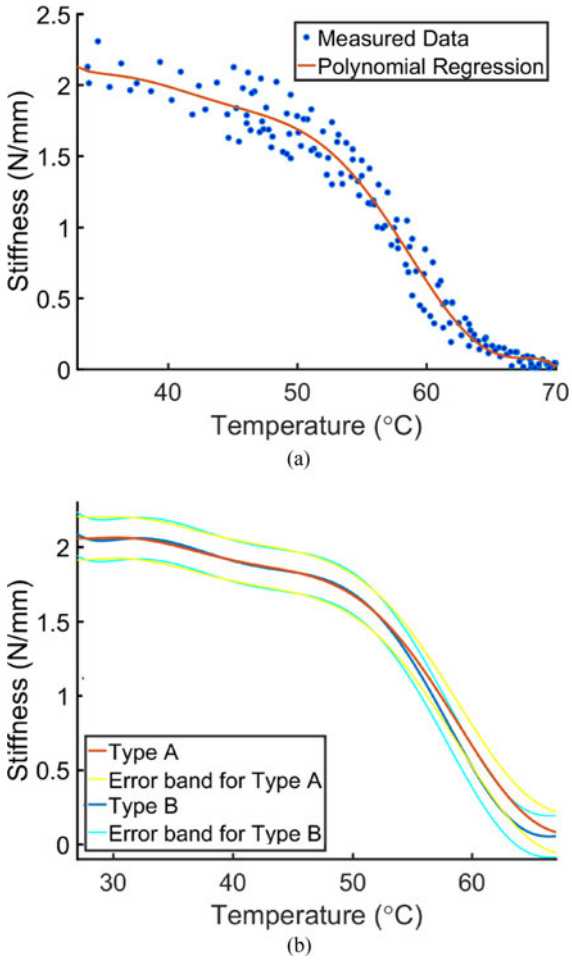

Fig. 5. (a) The relationship between stiffness and temperature of a typical Type A test piece shown by the measured data and 7th order polynomial fit. (b) The mean of polynmial fits for 25 tests performed across 5 samples of each type. Error bands representing one standard deviation

Fig. 5(b) shows the mean stiffness of both types of VS beam with respect to temperature. The Type A and Type B structures show similar behaviour. The structures can transition from a maximum stiffness of over $2\,\mathrm{N}\cdot\mathrm{mm}^{-1}$ to a minimum stiffness of less than $0.1\,\mathrm{N}\cdot\mathrm{mm}^{-1}$, representing over 95% reduction in stiffness. The error bands of each curve are also shown, which represent the standard deviation of all data from 5 different samples of each type and 5 tests of each sample (25 tests in all). The stiffness gradually reduces when temperature increases above 30 °C until about 50 °C, and it then rapidly reduces, approaching zero. This occurs near the glass transition temperature of pure PLA (60-65 °C) and GPLA (over 50 °C).

It should be considered that the measured temperature represents the surface temperature, which is expected to be lower than that of the central heating element, as heat loss occurs due to conduction, convection and radiation effects. Considerable reduction in stiffness across a short temperature range, in addition to repeatability of results and easy fabrication confirms the suitability of the technology for variable-stiffness purposes. Also, the VS beams demonstrate useful stiffness variation below their glass transition temperature. This may be a result of the internal sections of the beams being above T_g while the exterior is below it. Nonetheless, at these temperatures the beams behave elastically; they do not plastically deform and return to their initial position. Controllable variable-stiffness elastic behaviour is well suited for components in robotics, such as in walking, hopping and running robots.

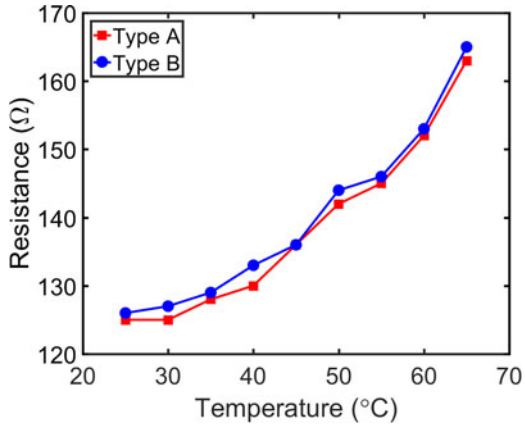

Fig. 6. The resistance-temperature relationship for both types (A and B) of the printed VS beams

A. *Variation of Electrical Resistance With Temperature*

Electrical resistance variation of the conductive GPLA embedded heating elements at various temperature was also investigated. To achieve this, the composite VS beam (Type A or Type B) was placed in a water bath. The resistance of the beam was measured when the sample was heated from 25 °C to 65 °C in increments of 5 °C. The resistivity of water does not affect the measurement significantly since it is much higher than the conductive GPLA lines, which were connected in parallel. As can be seen in Fig. 6, the electrical resistance of the structure increases as temperature increases. In future work, this resistance variation could be used as a sensing mechanism to infer temperature, although effects associated with geometry change would have to be accounted for.

B. *3D-Printed Variable-Stiffness Orthotic Structure*

To demonstrate the versatility and ready applicability of the presented 3D-printed variable-stiffness structures, a larger and more complex structure was designed and fabricated for use as a foot orthotic. A hexagonal honeycomb VS structure was printed as shown in Fig. 7. This structure weighed only 8.63 g (7.25 g PLA and 1.38 g conductive PLA) and measured 5 cm $\times$ 15 cm. Despite having lower density than the previous test samples (due to the open honeycomb design) it was strong enough to easily support a 200 g load (25 times greater than its own mass) in a horizontal beam configuration at room temperature (Fig. 7(c)). The open structure not only promotes faster heating and cooling, but also ensures breathability when used as a VS orthotic in contact with the skin. When the structure is heated by applying a voltage across the end connections it readily softens and bends under the applied load (Fig. 7(d)), demonstrating a considerable stiffness change.

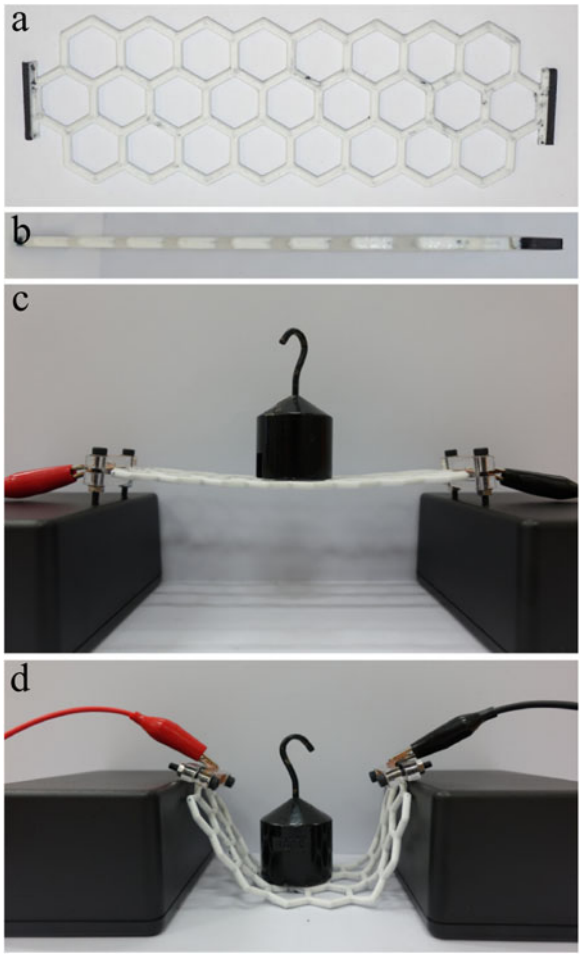

Fig. 7. (a) Top view, and (b) side view of the hexagonal VS structure suitable for orthotics, (c) 200 g mass supported by the VS sheet at room tempreture when no heating is applied; (d) after the application of current, the VS structure softens and deforms under the mass.

Foot drop is an inability to raise the front part of the foot due to weakness or paralysis of the tibialis anterior muscle that lifts the foot. The most common cause of spontaneous foot drop is peroneal neuropathy, which is often due to the compression of the fibular neck at the knee [19], [20]. The average mass of a foot is 1.33% of the total human mass [21], which is equivalent to around 1 kg for a 75 kg person. Ankle foot splints are commonly used to help patients keep their foot at the correct angle when they are walking. Our structure readily supported 200 g, suggesting a 1 kg supporting structure would be straightforward to manufacture.

The current 3D-printed VS structure can be readily adapted as a semi-active ankle orthosis. A larger piece (11 cm $\times$ 18 cm) was printed to demonstrate foot drop orthosis applications. Fig. 8(a) shows that the structure easily conforms to the shape of a foot when in its soft state and can be reshaped as needed simply by the application of electrical current. Wearing this orthotic sheet could help people who suffer from foot drop to keep their foot at the correct angle while walking so that the risk of tripping and challenges associated with step-climbing are reduced. In contrast to conventional rigid orthotic splints, the capability of

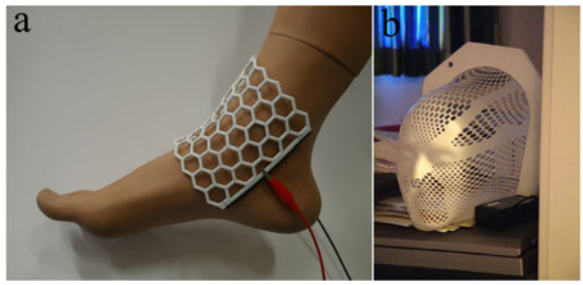

Fig. 8. (a) Foot drop orthosis electrically heated and shaped to fit the ankle; (b) radiotherapy mask which could be made of the PLA-GPLA VS technology.

the VS structure to easily transition between a rigid and soft state, would let the patient relax the foot in other conditions, for example when sitting. This is especially important to permit ankle movement (when not standing or walking) to promote blood circulation, a common problem for some people with diabetes.

Fig. 8(b) shows a typical radiotherapy mask, the wearing of which is needed during sessions of radiotherapy to the head. It ensures that the therapy is given in the correct location each time the patient returns for subsequent treatments. VS orthotics could be an appropriate solution for developing the next generation of these kind of masks. They could be printed either in a standard or custom 3D configuration (for example, the orthotic could be designed to exactly fit the patient's head, which could be measured with a 3D scanner), and could be reshaped as needed for comfort, modification, to accommodate surgical appendages or to ease mask removal. It is possible to design some parts of the structure so that they do not soften simply by using only non-conductive PLA, such that only chosen regions of the structure have the ability to be reshaped. It is worth noting that the orthosis and wearable structures might require thermal insulation to prevent skin discomfort, depending on the amount of stiffness change (and thus maximum temperature) required.

The low speed of stiffness change might limit the use of this technology in those applications that require high frequency stiffness variation. One solution could be always keeping the VS structure's temperature near its glass transition temperature so that by a small change in temperature, it can become considerably softer or harder. However, this method implies high energy costs since heat lost to the environment must be continuously replaced.

Quicker heating and cooling could be achievable by subjecting the structure to hot or cold air or liquid, either outside or inside heating and cooling channels, however this would add more complexity and mass to the entire structure. This research shows the requirement of basic material study to develop inexpensive thermoplastic polymers with lower glass transition temperatures, which could decrease both the energy and time required to achieve stiffness change. For example, polyurethane DiAPLEX shape memory polymer (SMP Technologies) has been used as a variable-stiffness material and its glass transition temperature can be tailored in a wide range (-40 to 120 °C) [7] However, for wearable technology, care should be taken in-case nearby body temperature triggers a change in stiffness.

An important point to consider is that as the VS structure exceeds its glass transition temperature, the material deforms in the plastic region rather than elastic region. In contrast, below the glass transition temperature behavior is elastic. It is also possible to exploit the shape-memory effect whereby the material can exert forces to return to its programmed shape at high temperatures. If it reaches a high enough temperature the polymer may be 'reprogrammed' into a new shape. These aspects of the technology will be the topic of study in future work.

IV. Conclusion

A new monolithic variable-stiffness structure made of both non-conductive PLA and graphene conductive PLA has been demonstrated. Arbitrary structures can be fabricated in a single-step using a low cost multi-material filament 3D printer. Heating the variable-stiffness structure above its glass transition temperature transitions it from a hard (rigid) state to a soft (rubbery) state. The stiffness of the VS beam can be reduced from over $2\,\mathrm{N}\cdot\mathrm{mm}^{-1}$ to a minimum stiffness of less than $0.1\,\mathrm{N}\cdot\mathrm{mm}^{-1}$, representing a reduction in stiffness of over 95%. 3D-printable conductive graphene PLA demonstrates promise as a heating element in this, and other robotic and orthotic structures. A lightweight VS sheet was printed in a breathable open honeycombed configuration to demonstrate the suitability of the technology for foot drop assistive orthotics. It can easily be shaped over the ankle and allows the patient to change the stiffness as desired. This letter represents the first demonstration of a 3D-printed monolithic, ready-to-use variable-stiffness structure. Future work will look at its controllability, speed of transition, cycle robustness, and application to other healthcare and soft robotic applications.

Acknowledgment

Data Access Statement: Data necessary to support conclusions are included in the article.

References

[1] I. K. Kuder, A. F. Arrieta, W. E. Raither, and P. Ermanni, "Variable stiffness material and structural concepts for morphing applications," *Prog. Aerosp. Sci.*, vol. 63, pp. 33–55, 2013.

[2] B. E. Schubert and D. Floreano, "Variable stiffness material based on rigid low-melting-point-alloy microstructures embedded in soft poly (dimethylsiloxane)(PDMS)," *RSC Adv.*, vol. 3, no. 46, pp. 24671–24679, 2013.

[3] N. G. Cheng *et al.*, "Design and analysis of a robust, low-cost, highly articulated manipulator enabled by jamming of granular media," in *Proc. 2012 IEEE Int. Conf. Robot. Autom.*, 2012, pp. 4328–4333.

[4] G. Tonietti, R. Schiavi, and A. Bicchi, "Design and control of a variable stiffness actuator for safe and fast physical human/robot interaction," in *Proc. 2005 IEEE Int. Conf. Robot. Autom.*, 2005, pp. 526–531.

[5] C. E. English and D. Russell, "Mechanics and stiffness limitations of a variable stiffness actuator for use in prosthetic limbs," *Mech. Mach. Theory*, vol. 34, no. 1, pp. 7–25, 1999.

[6] C.-A. Lahiff, T. Ramakrishnan, S. H. Kim, and K. Reed, "Knee orthosis with variable stiffness and damping that simulates hemiparetic gait," in *Proc. 2016 38th Annu. Int. Conf. IEEE Eng. Med. Biol. Soc.*, 2016, pp. 2218–2221.

[7] K. Takashima, J. Rossiter, and T. Mukai, "McKibben artificial muscle using shape-memory polymer," *Sens. Actuators A, Phys.*, vol. 164, no. 1, pp. 116–124, 2010.

[8] A. Y. N. Sofla, S. A. Meguid, K. T. Tan, and W. K. Yeo, "Shape morphing of aircraft wing: Status and challenges," *Mater. Des.*, vol. 31, no. 3, pp. 1284–1292, 2010.

[9] A. Loeve, P. Breedveld, and J. Dankelman, "Scopes too flexible . . . and too stiff," *IEEE Pulse*, vol. 1, no. 3, pp. 26–41, Nov./Dec. 2010.

[10] J. W. Hurst, J. E. Chestnutt, and A. A. Rizzi, "An actuator with physically variable stiffness for highly dynamic legged locomotion," in *Proc. IEEE Int. Conf. Robot. Autom.*, 2004, vol. 5, pp. 4662–4667.

[11] S. A. Migliore, E. A. Brown, and S. P. DeWeerth, "Novel nonlinear elastic actuators for passively controlling robotic joint compliance," *J. Mech. Des.*, vol. 129, no. 4, pp. 406–412, Apr. 2007.

[12] R. Van Ham, B. Vanderborght, M. Van Damme, B. Verrelst, and D. Lefeber, "MACCEPA, the mechanically adjustable compliance and controllable equilibrium position actuator: Design and implementation in a biped robot," *Robot. Auton. Syst.*, vol. 55, no. 10, pp. 761–768, Oct. 2007.

[13] M. Yalcintas and H. Dai, "Magnetorheological and electrorheological materials in adaptive structures and their performance comparison," *Smart Mater. Struct.*, vol. 8, no. 5, pp. 560–573, 1999.

[14] A. Tonazzini, A. Sadeghi, and B. Mazzolai, "Electrorheological valves for flexible fluidic actuators," *Soft Robot.*, vol. 3, no. 1, pp. 34–41, 2016.

[15] C. Liu, H. Qin, and P. T. Mather, "Review of progress in shape-memory polymers," *J. Mater. Chem.*, vol. 17, no. 16, pp. 1543–1558, 2007.

[16] T. P. Chenal, J. C. Case, J. Paik, and R. K. Kramer, "Variable stiffness fabrics with embedded shape memory materials for wearable applications," in *Proc. 2014 IEEE/RSJ Int. Conf. Intell. Robot. Syst.*, 2014, pp. 2827–2831.

[17] M. C. Yuen, R. A. Bilodeau, and R. K. Kramer, "Active variable stiffness fibers for multifunctional robotic fabrics," *IEEE Robot. Autom. Lett.*, vol. 1, no. 2, pp. 708–715, Jul. 2016.

[18] I. Pillin, N. Montrelay, and Y. Grohens, "Thermo-mechanical characterization of plasticized PLA: Is the miscibility the only significant factor?" *Polymer*, vol. 47, no. 13, pp. 4676–4682, Jun. 2006.

[19] F. Stevens, N. J. Weerkamp, and J. W. L. Cals, "Foot drop," *BMJ*, vol. 350, pp. 1–3, 2015.

[20] J. D. Stewart, "Foot drop: Where, why and what to do?" *Practical Neurol.*, vol. 8, no. 3, pp. 158–169, 2008.

[21] P. De Leva, "Adjustments to Zatsiorsky-Seluyanov's segment inertia parameters," *J. Biomech.*, vol. 29, no. 9, pp. 1223–1230, 1996.